Exciplex Photophysics. IV. Effect of Diffusion-Controlled Quenching on Exciplex Photokinetics

Man-Him Hui and William R. Ware*

Contribution No. 144 from The Photochemistry Unit, Department of Chemistry, University of Western Ontario, London, Ontario N6A 5B7, Canada.

Received December 1, 1975

Abstract: The influence of diffusion on the excimer or exciplex photokinetics has been investigated by numerical integration of the standard coupled differential equations for the situation where the forward quenching step has a time-dependent rate constant given by the continuum theory of diffusion-controlled reactions. The influence of diffusion on both the fluorescence decay and steady state behavior was investigated for a number of cases representative of typical exciplex systems. Methods of correction are discussed.

I. Introduction

It is well known that transient effects[1-3] associated with diffusion play an important role in a number of simple quenching systems.[2,4,5] These effects, however, have largely been ignored in excimer and exciplex systems although such systems have been under investigation for a number of years. A recent study[6,7] of the anthracene-*N*,*N*-dimethylaniline exciplex system demonstrated that the transient effect could be very large and should not be ignored even for nonviscous solvents like cyclohexane.

The present study is an attempt, through numerical calculation, to evaluate the importance of transient effects under a variety of conditions. A number of correction methods were critically tested in order to find suitable ways of correcting quenching data for these effects.

II. The Model

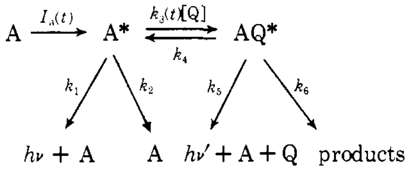

The reaction scheme used was the standard excimer type of mechanism[8] for nonpolar solvents with the exception that $k_3(t)$ was time dependent and given by the full diffusion rate equation.[1,2,3,5]

$$k_3(t) = \frac{4\pi RDN'}{1 + (D/\kappa R)}\left[1 + \frac{\kappa R}{D} e^{x^2} \operatorname{erfc}(x)\right] \tag{1}$$

where

$$x = \frac{\sqrt{Dt}}{(RD/[D + \kappa R])} \tag{2}$$

and

$$\operatorname{erfc}(x) = \frac{2}{\sqrt{\pi}} \int_x^\infty e^{-z^2}\, dz \tag{3}$$

R is the critical distance at which reaction takes place. D is the mutual diffusion coefficient between A* and Q.

$$D \equiv D_{AQ} = D_A + D_Q \tag{4}$$

and κ is the elementary reaction rate constant. The time dependence of k_3 is shown in Figure 1 for typical R, D, and κ.

There are various degrees of approximation to eq 1. In the zeroth order the time dependence is dropped altogether to give

$$k_3' = \frac{4\pi RDN'}{1 + (D/\kappa R)} = 4\pi R'DN' \tag{5}$$

where

$$R' = \frac{R}{1 + (D/\kappa R)} \tag{6}$$

Equation 5 in fact gives the limiting value of $k_3(t)$ as $t \to \infty$. The next degree of approximation gives

$$k_3'' = 4\pi R'DN'\left(1 + \frac{R'}{\sqrt{\pi Dt}}\right) \tag{7}$$

This equation is obtained by using the asymptotic expansion ($x > 1$)

$$e^{x^2} \operatorname{erfc}(x) = \frac{1}{x\sqrt{\pi}}\left(1 - \frac{1}{2x^2} + \frac{3}{4x^4} - \frac{15}{8x^8} + \ldots\right) \tag{8}$$

and retaining only the leading term. Thus

$$e^{x^2} \operatorname{erfc}(x) = 1/x\sqrt{\pi} \tag{9}$$

and eq 7 is obtained.

For ordinary values of κ, D, and R, it is found that k_3 and k_3'' are practically the same except for the first approximately 100 ps after δ-pulse excitation.

The reaction scheme gives rise to the following coupled first-order differential equations with time-dependent coefficients:

$$\frac{d[A^*]}{dt} = -(k_1 + k_2 + k_3(t)[Q])[A^*] + k_4[AQ^*] \tag{10a}$$

$$\frac{d[AQ^*]}{dt} = k_3(t)[Q][A^*] - (k_4 + k_5 + k_6)[AQ^*] \tag{10b}$$

These equations were solved numerically on the CDC Cyber 73/14 computer by means of Hamming's modified predictor corrector method. The particular subroutine employed was HPCG from IBM System/360 Scientific Subroutine Package.

The boundary conditions are for $t = 0$, $[A^*] = 1$, and $[AQ^*] = 0$, which yields the equivalent of the δ-pulse system response. The upper error bound, ϵ, was adjusted as follows:

[A*]	ϵ
10^0–10^{-2}	10^{-6}
10^{-2}–10^{-4}	10^{-7}
10^{-4}–10^{-6}	10^{-8}

The calculation began at $t_i = 0$ and continued to $t_f = 0.5$ μs or when either [A*] or [AQ*] fell below 10^{-6}.

[A*] and [AQ*] were then integrated numerically from t_i to t_f. The curves were then further integrated analytically to infinity assuming that the curves decayed exponentially to

Table I. Parameters Used in the Calculations

Case	τ_0, ns	k_4, μs^{-1}	k_p, μs^{-1}	R', Å	$D \times 10^5$, cm^2 s^{-1}	$4\pi R'DN'$, μs^{-1} M^{-1}
A	5.217	3.68	9.23	7	1.75	9.27
B	2	3.68	9.23	7	1.75	9.27
C	10	3.68	9.23	7	1.75	9.27
D	5.217	36.8	9.23	7	1.75	9.27
E	5.217	368	9.23	7	1.75	9.27
F	5.217	7.936	9.23	5.527.	4.78	19.99
G	5.217	0.427	9.23	8.126	0.175	1.076
H	18.5	0.150	110	4	4	12.11
I	18.3	4740	353	5.43	4.5	18.49

infinity with time constant equal to $\frac{1}{2}(\tau' + \tau'')$ where τ' is the apparent time constant at t_f and τ'' is the long-time constant (τ_2, see later section) when k_3 is constant. τ' and τ'' are essentially identical for all cases encountered.

In order to calculate $k_3(t)$ according to eq 1, the subroutine MERF (IMSL Library 3, 4th ed, International Mathematical and Statistical Libraries, Inc., 1974) was used to compute the complementary error function (eq 3). However, since erfc(x) is extremely close to zero when $x > 8$, eq 9 was used instead to compute the value of $k_3(t)$. At this x value, the values calculated according to eq 1 and 9 are well within 1%. However, the use of a different equation does create a slight discontinuity in $k_3(t)$. This occurs at a point when $k_3(t)$ is decreasing reasonably rapidly in value. Hence, no irregularities are apparent in [A*](t) or [AQ*](t) at this point.

III. Choice of Parameters

The necessary rate parameters of the kinetic scheme are completely described by the following variables: $\tau_0 = 1/(k_1 + k_2)$, k_4, $k_p = k_5 + k_6$, $R' = R/(1 + D/\kappa R)$, D, and κ. κ was calculated from gas kinetics using[1]

$$\kappa = k_{gas}/4\pi R^2 \tag{11}$$

with $k_{gas} = 10^{-10}$ cm^3 molecule^{-1} s^{-1}. Note that κ does not have the usual units of a rate constant. Nine different combinations of such parameters were used in the calculation, and these are shown in Table I.

Combination A represents the approximate condition of the anthracene-N,N-dimethylaniline system[6] in hexane at room temperature. Combinations B through G are all based on A. {B,A,C} represents an increase in τ_0. k_4 is increased in {A,D,E}. {F,A,G} represents a change in both $4\pi R'DN'$ and k_4 while keeping $4\pi R'DN'/k_4$ constant. Finally, H and I represent the "rapid equilibrium" situation of α-cyanonaphthalene and 1,2-dimethylcyclopentene in hexane.[8,9]

In each combination [Q] ranges from zero to approximately 1.25[Q]$_{1/2}$ where [Q]$_{1/2}$ is the quencher concentration at which $\Phi_M/\Phi_M{}^0 = \frac{1}{2}$.

IV. Tests for Accuracy

The IBM/360 Scientific Subroutine Package claims that "numerical experience seems to show that the procedure does not exceed a global relative error approximately equal to ϵ". With the ϵ values used in this calculation, the accuracy is thus more than enough for our purpose.

An independent method was used to test the accuracy of the procedure. When k_3 is constant, eq 10 can of course be solved analytically. The procedure was applied to a situation in which the rates are similar to case A with the exception that k_3 was kept constant at $4\pi R'DN'$. The result obtained was compared with that obtained by numerical integration of eq 10. It was found that at $t_f = 0.5$ μs, the error in [A*] was 1.3 ppm and that in [AQ*] was 0.35 ppm. The error in integration to infinity was slightly larger. The area under the [A*](t) curve had an error of 0.02% while the error for the [AQ*] curve was 0.008%. This is clearly satisfactory for the purpose at hand.

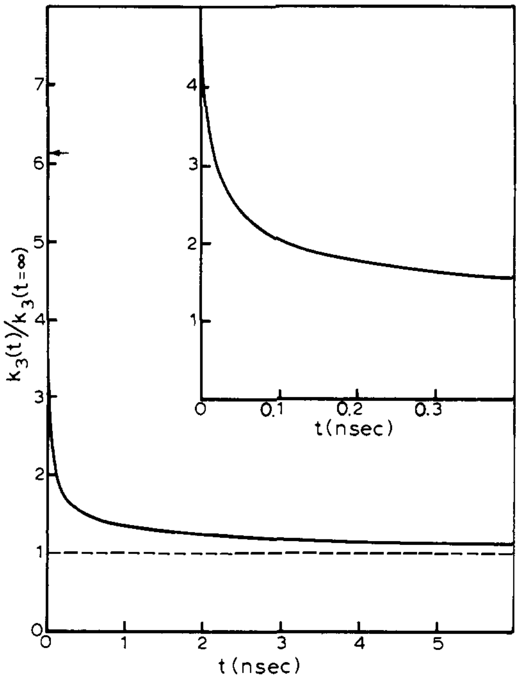

Figure 1. Plot of eq 1 as $f(t)$ for $D = 1.62 \times 10^{-5}$ cm^2 s^{-1}, $R = 9.55$ Å, $R' = 8$ Å, $\kappa = k_{gas}/4\pi R^2$, and $k_{gas} = 10^{-10}$ cm^3 molecule^{-1} s^{-1}. Insert: expansion of the plot from 0 to 0.4 ns.

V. Results and Discussion

The numerical calculation generated [A*], [AQ*], and the areas under these two functions. [A*] and [AQ*] are the time responses of the system to δ-pulse excitation, while the areas under [A*] and [AQ*] give a measure of Φ_M and Φ_E, respectively. Hence, the Stern-Volmer curve ($\Phi_M{}^0/\Phi_M$ vs. [Q]) and Φ_E/Φ_M vs. [Q] curves can be readily generated.

The special concern of this work is to examine what sort of discrepancies occur in the above-mentioned data ([A*], [AQ*], $\Phi_M{}^0/\Phi_M$ vs. [Q], and Φ_E/Φ_M vs. [Q]) when transient effects come into play.

When k_3 is constant ($= 4\pi R'DN'$), the following equations result.[3,6,7]

$$[A^*] = C_1 e^{-\lambda_1 t} + C_2 e^{-\lambda_2 t} \tag{12}$$

$$[AQ^*] = C_3(e^{-\lambda_1 t} - e^{-\lambda_2 t}) \tag{13}$$

where

$$C_1 = \frac{\lambda_1 - k_4 - k_p}{\lambda_1 - \lambda_2}[A^*]_0 \tag{14}$$

$$C_2 = \frac{k_4 + k_p - \lambda_2}{\lambda_1 - \lambda_2}[A^*]_0 \tag{15}$$

and

$$C_3 = -\frac{k_3[Q]}{\lambda_1 - \lambda_2}[A^*]_0 \tag{16}$$

$$1/\tau_{1,2} \equiv \lambda_{1,2} = \tfrac{1}{2}\{k_1 + k_2 + k_3[Q] + k_4 + k_p \pm \sqrt{(k_1 + k_2 + k_3[Q] - k_4 - k_p)^2 + 4k_3k_4[Q]}\} \tag{17}$$

In addition, for the steady state the following equations apply[3,6,7]

$$\Phi_M{}^0/\Phi_M = 1 + \left(\frac{k_3}{k_1 + k_2}\right)\left(k_p/k_4 + k_p\right)[Q] \tag{18}$$

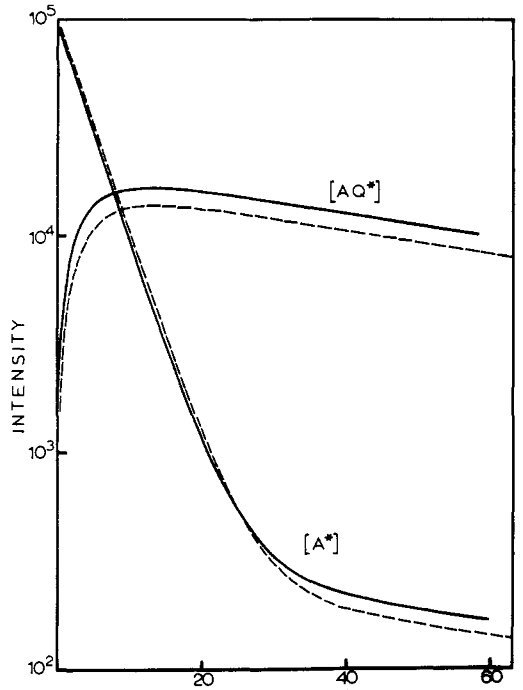

Figure 2. (—) Numerically generated [A*] and [AQ*] based on $k_3(t)$. (- - -) Limiting case of $k_3 = 4\pi R'DN'$. Case A, Table I, [Q] = 0.004 07 M.

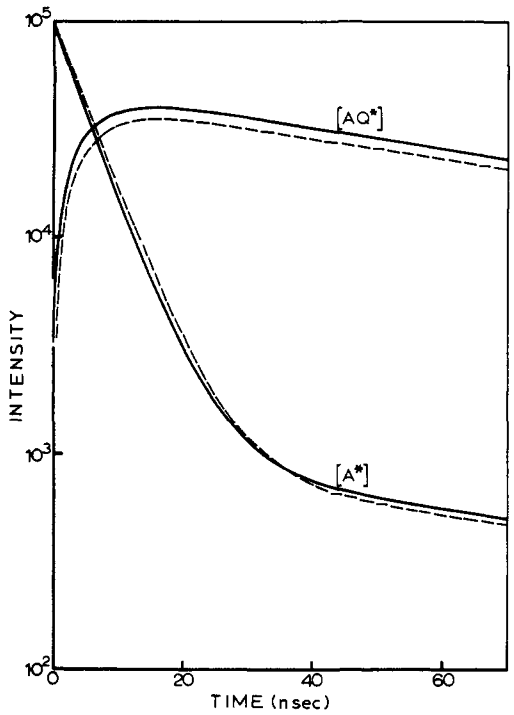

Figure 4. (—) Numerically generated [A*] and [AQ*] based on $k(t)$. (- - -) Limiting case of $k_3 = 4\pi R'DN'$. Case C, Table I, [Q] = 0.008 14 M.

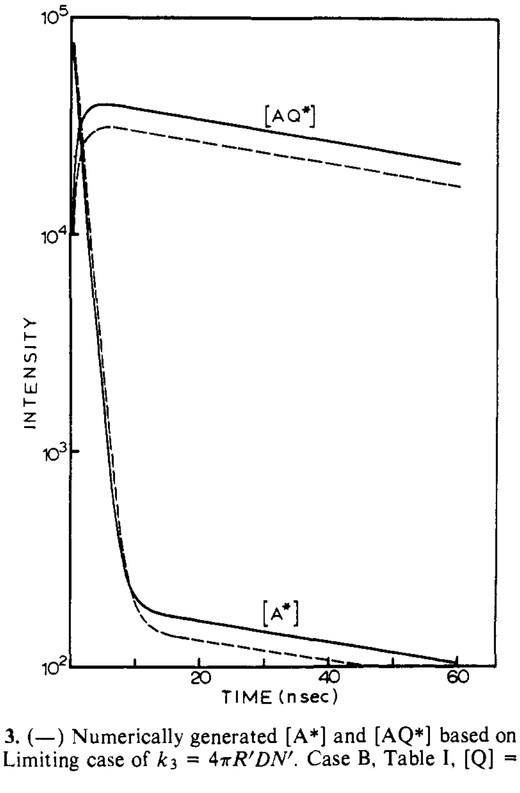

Figure 3. (—) Numerically generated [A*] and [AQ*] based on $k_3(t)$. (- - -) Limiting case of $k_3 = 4\pi R'DN'$. Case B, Table I, [Q] = 0.027 M.

$$\Phi_E/\Phi_M = \frac{k_3}{k_4 + k_p}[Q] \qquad (19)$$

[note that Φ_E/Φ_M is defined here in a different manner than in earlier publications[6,8]]. The question is, how well do these equations describe the system when k_3 is no longer time independent?

For example, can [A*] and [AQ*] be represented by a sum and difference of exponentials? Are the τ_1 and τ_2 values in [A*] the same as those in [AQ*]? Do the coefficients C_1, C_2, and C_3 bear any relation to those predicted by eq 14–16? If one writes [AQ*] as $A_1e^{-t/\tau_1} + A_2e^{-t/\tau_2}$, is $A_1 = -A_2$?

Equation 18 predicts the Stern-Volmer plots to be linear. On the other hand, in simple quenching systems (no exciplex formation) in the presence of transient effects the line usually curves upwards with magnitude of the curvature dependent on the importance of the transient effect.[4,5] In the present cases, is the line straight or curved? Similarly, what about the Φ_E/Φ_M curve? Also, is there a suitable method to analyze the decay curves and a suitable way to correct the steady state data for transient effects?

There are several assumptions implicit in this kinetic treatment. (a) The initial distribution of A and Q is random. (b) One can ignore the dissociation of AQ* to regenerate A* and Q as neighbors. Assumption (a) has been discussed at length in an earlier publication.[5] The point in question is merely the influence of ground state complexing. Assumption (b) appears safe for complexes with lifetimes significantly longer than the time required for k_3 to reach, say, 90% of its steady state value. The possibility of recombination of the A*-Q pair is included in the value of k_4 found necessary to account for the kinetic data behavior.

(a) Behavior of [A*]. In general [A*], generated from eq 10, decays with a shape qualitatively corresponding to the sum of two exponentials. However, a direct comparison reveals that [A*] initially falls more rapidly than predicted by eq 12 and then decays with the same long-time constant. Direct comparison can be made by taking $k_3 = 4\pi R'DN'$ for the evaluation of eq 12, and otherwise using the same parameters in the solutions of eq 10 and the generation of the decay by eq 12. When this is done, the [A*] from eq 10 crosses that predicted by eq 12 and both decay with the same long-time constant. At long time [A*] from eq 10 is displaced above that predicted by eq 12. This is illustrated in Figures 2, 3, and 4 for cases A, B, and C. The above remarks apply to the case where the exciplex lifetime is considerably longer than the time required for k_3 to reach 90% of its steady state value (a few nanosec-

Table II. Results of Numerical Integration of the Coupled Exciplex Differential Equations

Case	Shape of $[A^*](t)$	$R'/\sqrt{\tau_0 D}$, %	K_{SV}	$k_3\tau_0 \times \frac{k_p}{k_4 + k_p}$	R_M	$\frac{d}{d[Q]} \times \left(\frac{\Phi_E}{\Phi_M}\right)$	$\frac{k_3}{k_4 + k_p}$	R_E	$k_3\tau_0 \times \left(\frac{k_p}{k_4 + k_p}\right) \times \left(1 + \frac{R'}{\sqrt{\tau_0 D}}\right)$	K_{SV}^0
A	Analyzable	23.2	44.77	34.58	1.30	936.8	718.1	1.31	42.59	42.15
B	Barely analyzable	37.4	19.19	13.26	1.45	1052	718.1	1.47	18.22	17.86
C	Analyzable	16.7	81.74	66.28	1.23	895.0	718.1	1.25	77.37	77.0
D	Barely analyzable	23.2	11.49	9.699	1.19	237.9	201.4	1.18	11.95	11.75
E	Not analyzable, τ_1 too short, undershoot	23.2	1.289	1.184	1.09	26.53	24.58	1.08	1.46	1.39
F	Analyzable	11	63.23	56.09	1.12	1314	1165	1.13	62.30	61.6
G	Barely analyzable	85	11.98	5.37	2.23	257.4	111.4	2.31	9.93	9.85
H	Not analyzable, τ_1 too short, C_1 too small	46	100.9	94.78	1.06	49.72	46.57	1.07	99.05	99.18
I	Not analyzable, τ_1 too short, C_1 too small	6.0	25.37	23.46	1.08	3.942	3.631	1.09	24.86	24.82

onds) and the monomer quenched decay time is of the order of 2–10 ns.

It was considered of interest to examine the influence of the time dependence of k_3 when the decay was forced to fit a double exponential. That is, what errors are encountered in λ_1 and λ_2 for various sets of rate constants and quencher concentrations?

In order to examine this question, data were generated by two different techniques. In the first, $[A^*]$ from the solution to eq 10 was convoluted with a typical lamp (which incorporated photomultiplier distortion)[10,11] and the resultant curve normalized to 10^5 counts. Gaussian noise was then added. This represents in a rather realistic manner the type of decay curve obtained from the single photon technique.[10-12] In the second method, $[A^*]$ was normalized to 10^5 counts without convolution, and Gaussian noise then added. These decay data represent what one would obtain with a single photon instrument of infinite time resolution with a δ pulse of light.[10,11]

The decay curves generated by convolution with a typical lamp were then deconvoluted by iterative convolution[10,11] assuming an instantaneous fluorescence response function $C_1 \exp(-\lambda_1 t) + C_2 \exp(-\lambda_2 t)$. In general when the monomer curve was analyzed from the initial point on the rising edge, the fit to the double exponential was poor ($\chi^2 \gg 1$).[13] If the starting point for the iterative convolution was gradually shifted to longer times beyond the maximum, the fit improved, λ_1 became smaller and approached the value predicted by eq 17, whereas the λ_2 became constant and agreed with that obtained from the analysis of the $[AQ^*]$ decay (vide infra). The pre-exponential factors also changed and approached constant values as λ_1 and λ_2 approached their limiting values.

Thus meaningful values for λ_1 and λ_2 can be obtained provided the short-lived component of the monomer decay curve is long compared with the time evolution of k_3, and provided C_1 is not too small. As the decay time of the short component approaches the time required for k_3 to reach, say, 90% of its steady state value, it is no longer possible to obtain an iterative two-component fit working only on the trailing edge of the decay at some distance from the maximum.

These observations are summarized in Table II. In this table the notation "analyzable" means that the curve behaves normally in the sense that if one omits the initial portion of the decay one can recover the λ_1 and λ_2 that pertain to the situation where k_3 has reached its steady state value. It was found that this can be done to within a few percent error.

Table II contains a number of cases which are not "analyzable" and the reasons are indicated in the table. The rate constants responsible for this state of affairs can be found in Table I.

Cases A and B were also examined to determine the validity of the frequently used equation[3,8,9]

$$\lambda_1 + \lambda_2 = k_1 + k_2 + k_3[Q] + k_4 + k_p \qquad (20)$$

which is the standard route to k_3. The only difference between cases A and B is that in the latter the unquenched lifetime is quite short (2 ns vs. 5 ns). $k_3(t)$ was the same in both cases. The results were as follows. In case A, the values of k_3 were on the average 3% too high. k_3 obtained from eq 20 was 9.5 ± 1.2 ns^{-1} M^{-1} whereas $4\pi R'DN'$ was 9.27 ns^{-1} M^{-1}. Thus the error in establishing the steady state k_3 was only 2.5%. In case B where the forced fit to two exponentials is less successful, eq 20 gives $k_3 = 10.96 \pm 1.27$ ns^{-1} M^{-1} whereas $4\pi R'DN'$ was again 9.27 ns^{-1} M^{-1}. The error is 18%, and of course as the unquenched lifetime is decreased further the error will increase and the fit to two exponentials will further deteriorate.

Under certain circumstances (case E, for example, with large k_4), the decay of $[A^*]$ exhibits a pronounced undershoot. $[A^*]$ initially drops rapidly, then it recovers, passes through a slight maximum, and then decays again to give a long component with λ_2 equal to the input λ_2. This is illustrated in Figure 5 for case E. This is not due to the almost insignificant discontinuity in $k_3(t)$ described above (in the evaluation of $x^2 \operatorname{erfc}(x)$) and appears to be a real effect. The explanation is merely that the decay of $[A^*]$, the growth of $[AQ^*]$, and the time dependence of $k_3(t)$ combine to give over a short period of time a net increase in $[A^*]$ from feedback. The sign of $d[A^*]/dt$ was checked using eq 10 and at the point in time where $[A^*]$ is increasing one indeed has a positive derivative using the parameters for case E.

In cases where it is possible to recover λ_1 and λ_2 by judicious choice of deconvolution limits, we can then recover all the rate constants by one of several methods. See, for example, papers I, III, and IV of this series.[6,8,9]

(b) Behavior of $[AQ^*]$. The temporal behavior of $[AQ^*]$ also departs from what one would expect on the basis of a time-independent k_3. $[AQ^*]$ in fact rises much more rapidly than expected from eq 13. If a comparison is made using $k_3 = 4\pi R'DN'$ for k_3 in eq 13 and otherwise the same parameters in eq 10 and eq 13, one observes that the initial faster rise is followed by a displacement such that the plot of eq 13 lies below that of the solutions to eq 10. The two eventually parallel

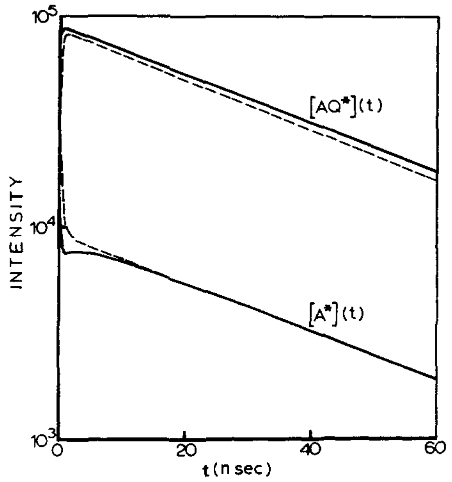

Figure 5. (—) Numerically generated [A*] and [AQ*] based on $k(t)$. (- - -) Limiting case of $k_3 = 4\pi R'DN'$. Case E, Table I, [Q] = 0.344.

one another as would be expected once $k_3(t)$ has become essentially constant. This is illustrated in Figures 2, 3, and 4. Also, a time-dependent k_3 causes the coefficients in $C_3'e^{-\lambda_1 t} - C_3''e^{-\lambda_2 t}$ to be of unequal magnitude. While one still gets a growth and subsequent decay, [AQ*] is no longer described by $C_3[\exp(-\lambda_1 t) - \exp(-\lambda_2 t)]$.

[AQ*] remains useful for determining rate constants in the presence of significant effects attributable to $k_3(t)$ only insofar as one can establish the long lifetime from that portion of the decay well past the maximum. It appears that the error here is negligible unless the exciplex is quite short lived. To attempt to obtain the short lifetime requires inclusion in the deconvolution of that portion of the decay leading up to the maximum and for the cases listed in Table I this approach is hopeless, and a different approach is required. It should be recognized that with a more general analysis the rising edge of [AQ*] can potentially yield R and κ.[7]

(c) Steady State. As described above, the steady-state ratios $\Phi_M/\Phi_M{}^0$ and Φ_E/Φ_M were obtained by integrating decay laws to infinity. The resultant Stern-Volmer plots were in general slightly curved upwards but this curvature was so slight as to probably escape detection even in measurements of rather high precision (1-2%). The Φ_E/Φ_M vs. [Q] plots parallel the behavior exhibited by the Stern-Volmer plots in the sense that there is slight upward curvature.

Thus for the cases given in Table I, the steady-state data can be treated as linear to an excellent approximation. For both $\Phi_M/\Phi_M{}^0$ and Φ_E/Φ_M vs. [Q], the slopes obtained were always considerably greater than predicted by eq 18 and eq 19 when k_3 was taken as $4\pi R'DN'$. In some cases the discrepancy was very large (750%).

It is helpful at this point to define a quantity which gives a measure of the transient effect in various cases. A useful parameter appears to be given by[1-5] $\xi = R'/\sqrt{\tau_0 D}$. In the simplest quenching system (no exciplex, with constant $k_3 = 4\pi R'DN'$) the Stern-Volmer equation is

$$\Phi_M{}^0/\Phi_M = 1 + k_q\tau_0[\mathrm{Q}] \qquad (21)$$

On the other hand, when diffusion effects are taken into account by assuming k_q to be given by eq 7, the following can be derived:

$$\lim_{[\mathrm{Q}]\to 0}\left(\frac{\Phi_M{}^0}{\Phi_M}\right) = 1 + k_q\tau_0\left(1 + \frac{R'}{\sqrt{\tau_0 D}}\right)[\mathrm{Q}] \qquad (22)$$

Hence, ξ can be used as a measure of the transient effect. Of course, eq 7 is not as exact as eq 1 (k_q is overemphasized in the initial 100 ps or so). ξ does, however, give an indication of the transient effect due to diffusion.

The following correction methods for steady state data were examined.

Method A. Equations 18 and 19 can be rewritten as

$$(\Phi_M{}^0/\Phi_M - 1) = k_3\tau_0\left(\frac{k_p}{k_4 + k_p}\right)[\mathrm{Q}] \qquad (23)$$

$$\frac{\Phi_E}{\Phi_M} = \left(\frac{k_5}{k_1}\right)\left(\frac{k_3}{k_4 + k_p}\right)[\mathrm{Q}] \qquad (24)$$

These two equations are correct if k_3 is constant. Since in all nine cases studied the steady state plots were reasonably straight, it is therefore possible to represent the data empirically as:

$$\left(\frac{\Phi_M{}^0}{\Phi_M} - 1\right) = k_3\tau_0\left(\frac{k_p}{k_4 + k_p}\right)[\mathrm{Q}] \qquad (25)$$

$$\frac{\Phi_E}{\Phi_M} = \frac{k_5}{k_1}\frac{k_3}{k_4 + k_p}[\mathrm{Q}] \qquad (26)$$

The question is whether or not k_3 in both eq 25 and 26 is the same.

In Table II, the following are listed: (a) K_{SV} = the slope of the Stern-Volmer curve; (b) $k_3\tau_0\,[k_p/(k_4 + k_p)]$ = expected slope if there is no transient effect; (c) $R_M = K_{SV}/k_3\tau_0(k_p/[k_4 + k_p])$; (d) d/d[Q] (Φ_E/Φ_M) = slope of Φ_E/Φ_M vs. [Q] curve; (e) $k_3/(k_4 + k_p)$ = expected slope, divided by known (k_5/k_1), in the absence of diffusion transient effect; (f) R_E = d/d[Q] $(\Phi_E/\Phi_M)/[k_3/(k_4 + k_p)]$. If k_3 in eq 25 and 26 is the same, R_M would be equal to R_E. Indeed, as shown in Table II the two numbers are very close in all nine cases. Therefore, this is a valid and very useful correction method.

Another observation is that diffusion effects are always present even in case H (6%) which represents approximately the system α-cyanonaphthalene and 1,2-dimethylcyclopentene in hexane at room temperature. Also, note that in case G, the discrepancy in the slope is very high (123%).

This method, though accurate, is not applicable at all times since to use this approach $k_3 = 4\pi R'DN'$, τ_0, k_4, and k_p must be known. One way is to obtain these parameters from kinetic data (anthracene-*N*,*N*-dimethylaniline case). But as mentioned in the last section, accurate determination of the steady state k_3 is not always possible.

Method B. When there is no exciplex formation and no diffusion effect,

$$K_{SV} = \left(\frac{\Phi_M{}^0}{\Phi_M} - 1\right)\left(\frac{1}{[\mathrm{Q}]}\right) = k_q\tau_0 \qquad (27)$$

If the effect of diffusion is added (using eq 7),

$$\lim_{[\mathrm{Q}]\to 0}(K_{SV}) = K_{SV}{}^0 = k_q\tau_0\left(1 + \frac{R'}{\sqrt{\tau_0 D}}\right) \qquad (28)$$

For the exciplex system without diffusion effects,

$$K_{SV} = k_3\tau_0\left(\frac{k_p}{k_4 + k_p}\right) \qquad (29)$$

Equations 27-29 naturally suggest one try the following:

$$K_{SV}{}^0 = k_3\tau_0\left(\frac{k_p}{k_4 + k_p}\right)\left(1 + \frac{R'}{\sqrt{\tau_0 D}}\right) \qquad (30)$$

To check the validity of the equation

$$k_3\tau_0\left(\frac{k_p}{k_4 + k_p}\right)\left(1 + \frac{R'}{\sqrt{\tau_0 D}}\right)$$

and $K_{SV}{}^0$ values were calculated and listed in Table II. The two numbers are indeed always very close to one another. Therefore, this correction method is reasonably accurate. On the other hand, this method requires the knowledge or estimate of D and R'.

It is also noteworthy that the

Table III. Rapid Equilibrium Case

k_p, ns^{-1}	k_3/k_4	Recovered k_p	Recovered k_3/k_4
0.353	3.90	0.368	3.58

$$k_3\tau_0\left(\frac{k_p}{k_4+k_p}\right)\left(1+\frac{R'}{\sqrt{\tau_0 D}}\right)$$

value, though close to $K_{SV}{}^0$, is always slightly larger. This is probably due to the fact that eq 7 instead of eq 1 was used to derive the correction factor. Since eq 7 overemphasizes $k_3(t)$ especially at short times, the correction factor is probably slightly too large.

(d) Rapid Equilibrium Case. [A*] and [AQ*] were generated in the usual manner from eq 10 using the parameters of case I.[8,9] Ln [A*] is essentially a straight-line function of time except for the initial 1 or 2 ns. The ln ([A*]) vs. t curves were analyzed as straight lines from 10 ns beyond the beginning of the curve to give $\tau = 1/\lambda$. Typical results are shown in Figure 6 for case I. It is easily shown that

$$(\lambda-\lambda_0)^{-1}=\frac{1}{k_p-\lambda_0}+\frac{1}{(k_p-\lambda_0)k_3/k_4}[\mathrm{Q}]^{-1}$$

where λ_0 pertains to [Q] = 0.

$(\lambda-\lambda_0)^{-1}$ was plotted against $[\mathrm{Q}]^{-1}$. The slope gives $1/(k_p-\lambda_0)$ and intercept $1/(k_p-\lambda_0)k_3/k_4$. Since $\lambda_0 = 1/\tau_0$ was known, k_p and k_3/k_4 could be calculated.

In the Table III, k_p and k_3/k_4 were the input numbers for the numerical calculation, where $k_3 = 4\pi R'DN'$, and R' and D are as given in Table I, case I. Recovered k_p and k_3/k_4 are the values obtained from the above procedure. Thus there are small but significant errors even when $\tau_0 \cong 20$ ns.

The ultimate goal in the analysis of quenching systems thought to involve exciplexes is to examine the validity of various kinetic schemes and then establish rate constants and temperature coefficients as a function of solvent, quencher, etc. Unfortunately, the systems in question can be completely described by no less than six rate constants (and in polar solvents probably seven are required). Two can be obtained from the unquenched monomer and k_5 and k_6 can be combined without the loss of essential information. However, k_3 is a function of D, R, and κ and even if D is known accurately one has in general four unknowns: k_4, k_p, R, and κ. One possibility for a more general solution to the problem posed in this paper would be to search for a minimum in the resultant four-dimensional χ^2 surface generated by comparing monomer or exciplex curves with those computed by convolution of numerical solutions to eq 10 with the instrumental response function[11,12] appropriate to the data at hand. This would probably be both expensive in computer time and prone to problems associated with noise in the data[11] and would furthermore require a rather good initial guess if it was successful at all. The treatment in this paper could provide the starting point for such a calculation.

The sensitivity of the fit to the uncertainty in D would also require investigation. This approach has not been investigated in the present research but may have considerable merit.

VI. Conclusions

This study shows that transient effects associated with diffusion can be very large indeed and should never be neglected. The effect on decay data is relatively less serious and can be avoided in some cases. On the other hand, the effect on steady state measurements is very large. The correction methods suggested are reasonably accurate but are not free from problems. On the whole, the picture is not very encouraging because only in certain cases can rate constants be recovered accurately.

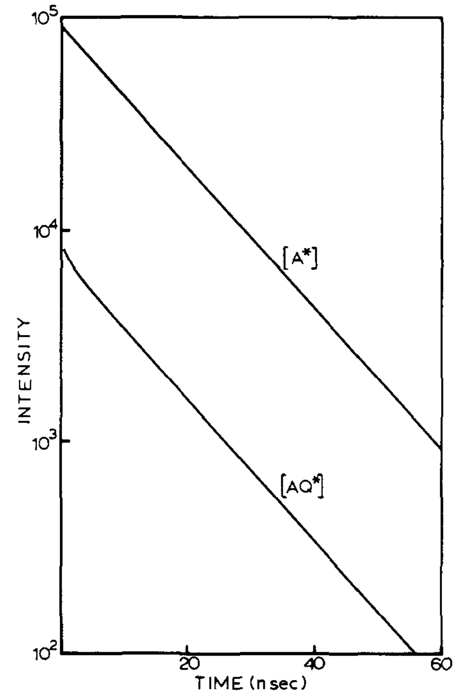

Figure 6. The rapid equilibrium limit (case I, Table I). [Q] = 0.0212 M. Lines calculated from eq 10 for $k_3 = f(t)$.

The analysis presented here may be considered a useful preliminary to a more rigorous analysis, even when only rough estimates of rate constants result.

Acknowledgments. The authors wish to acknowledge the support of the National Research Council of Canada for support of this work.

References and Notes

(1) R. M. Noyes, *Prog. React. Kinet.*, **1**, 129 (1961).
(2) A. Weller, *Z. Phys. Chem.* (*Frankfurt am Main*), **13**, 335 (1957).
(3) H. Beens and A. Weller, "Organic Molecular Photophysics", Vol. II, J. B. Birks, Ed., Wiley-Interscience, New York, N.Y., 1973, Chapter 4. A. H. Alwattar, M. D. Lumb, and J. B. Birks, *ibid.*, Vol. I, 1973, pp 403–454.
(4) W. R. Ware and J. Novros, *J. Phys. Chem.*, **70**, 3246 (1966).
(5) W. R. Ware and T. L. Nemzek, *J. Chem. Phys.*, **62**, 477 (1975).
(6) M. H. Hui and W. R. Ware, *J. Am. Chem. Soc.*, following paper in this issue.
(7) T. J. Chuang and K. B. Eisenthal, *J. Chem. Phys.*, **62**, 2213 (1975); **59**, 2140 (1973).
(8) W. R. Ware, D. Watt, and J. D. Holmes, *J. Am. Chem. Soc.*, **96**, 7853 (1974). Paper I of this series.
(9) D. V. O'Connor and W. R. Ware, preceding paper in this issue.
(10) H. Beens and A. Weller, *Acta Physiol. Pol.*, **34**, 85 (1968); D. Rehm and A. Weller, *Isr. J. Chem.*, **8**, 259 (1970); H. Knibbe, Thesis, University of Amsterdam, 1969.
(11) W. R. Ware, L. J. Doemeny, and T. L. Nemzek, *J. Phys. Chem.*, **77**, 2038 (1973).
(12) C. Lewis, W. R. Ware, L. J. Doemeny, and T. L. Nemzek, *Rev. Sci. Instrum.*, **44**, 107 (1973).
(13) χ^2 is used here with its usual statistical significance. See, for example, P. R. Bevington, "Data Reduction and Error Analysis For the Physical Sciences", McGraw-Hill, New York, N.Y., 1969.